ISSN 0030-400X, Optics and Spectroscopy, 2016, Vol. 120, No. 6, pp. 864–870. © Pleiades Publishing, Ltd., 2016.

SPECTROSCOPY OF ATOMS AND MOLECULES

# EIT Resonance Features in Strong Magnetic Fields in Rubidium Atomic Columns with Length Varying by 4 Orders[1]

**R. Mirzoyan[a], A. Sargsyan[a], D. Sarkisyan[a], A. Wojciechowski[b], A. Stabrawa[b], and W. Gawlik[b]**

[a] *Institute for Physical Research, NAS of Armenia, Ashtarak, 0203, Armenia*
[b] *Department of Photonics, M. Smoluchowski Institute of Physics, Jagiellonian University, 30–348 Kraków, Poland*
*e-mail: davsark@yahoo.com*

Received July 15, 2015; in final form, January 12, 2016

**Abstract**—Electromagnetically induced transparency (EIT) resonances are investigated with the $^{85}$Rb $D_1$ line (795 nm) in strong magnetic fields (up to 2 kG) with three different types of spectroscopic vapor cells: the nano-cell with a thickness along the direction of laser light $L \approx 795$ nm, the micro-cell with $L = 30$ μm with the addition of a neon buffer gas, and the centimeter-long glass cell. These cells allowed us to observe systematic changes of the EIT spectra when the increasing magnetic field systematically decoupled the total atomic electron and nuclear angular moments (the Paschen-Back/Back-Goudsmit effects). The observations agree well with a theoretical model. The advantages and disadvantages of a particular type of cell are discussed along with the possible practical applications.

**DOI:** 10.1134/S0030400X16060151

## INTRODUCTION

Coherent interaction of light fields with three-level atomic/molecular systems is responsible for such widely studied processes as coherent population trapping (CPT) and electromagnetically induced transparency (EIT). These processes find many exciting applications in fundamental and applied science: in metrology, magnetometry, quantum communication, atomic clocks, etc. [1–5]. In particular, EIT resonances in strong magnetic fields allow one to form tunable narrow optical reference resonances (displaced by several GHz) from the unperturbed atomic transitions. This can be used in laser frequency stabilization, which is often necessary in practice [6], and also for the construction of secondary tunable frequency references with a spectral resolution of a few MHz.

A small number of papers on EIT in strong magnetic fields $B \sim 1$ kG is caused mainly by the difficulty of creating strong, sufficiently homogeneous magnetic fields in several-cm-long cells, filled with vapor of alkali metal atoms. Because of these technical problems, previous studies of EIT in Rb vapor cells were limited to fields not exceeding 40–50 G [7, 8]. While modern permanent magnets (PM) can create a field of several kG at distances of several centimeters, they are usually strongly inhomogeneous (field gradients reaching 100 G/mm), which excludes their application with centimeter-long cells. On the other hand, the problem of field inhomogeneity may be alleviated by application of vapor columns of micrometer or submicrometer thickness.

In [9], EIT in $^{87}$Rb $D_1$ line under strong magnetic fields was investigated using nano-cell (NC) with the vapor column length $L = \lambda = 795$ nm. At low magnetic field $B$ three EIT-resonances were recorded, however for $B > 1.2$ kG only one resonance was visible.

In the present paper, a modification of the EIT spectra of the $D_1$ line of $^{85}$Rb atoms in strong magnetic field is systematically investigated for the first time with three cells of very different lengths: the nano-cell (NC) with $L \approx \lambda \approx 795$ nm, the micro-cell (MC) with $L \approx 30$ μm, and the centimeter-cell with $L \approx 1$ cm. We also present EIT spectra in 0.8 and 2.5 cm-long cells placed in a homogenous magnetic field and compare them with those observed in NC. This comparative study aims at determination of optimum cell design for registration of the EIT resonances in strong magnetic fields.

## EXPERIMENT

### *Nano-cell*

The nano-cell used in this work was described previously [10]. It allows one to vary smoothly the atomic vapor column thickness in the range of 100–1200 nm

[1] The article is published in the original.

in the vertical direction. Its rectangular windows with size of 25 × 30 mm and 2 mm thick are made of carefully polished crystal sapphire (roughness is of ~5 nm), with an axis C perpendicular to the window surface to reduce birefringence. To form a tapered gap between the inner surfaces of the windows, a platinum strip of 1.2 μm thickness is placed at the bottom of NC. The side-arm of the NC is filled with natural Rb. The NC enables using relatively large light beams area (about 1 × 1 mm) along a constant cell length of $L \sim \lambda = 795$ nm. The deviation of the gap thickness from this value is below ±10% and does not deteriorate the EIT resonance parameters. The heating oven for the NC and MC is made of non-magnetic material and has two openings for passage of the laser beam. The oven consists of two heaters: the first one for heating of the windows, and the second one for the side arm (SA), where the Rb is stored. SA temperature is 120°C, which provides a vapor density of $N \sim 2 \times 10^{13}$ cm$^{-3}$. To prevent condensation of Rb on the NC windows their temperature is kept about 20°C above the SA temperature. For the selection of the required cell-gap thickness $L \approx \lambda$, the oven with NC was attached to a vertically movable nonmagnetic table (for details, see [11]).

### *Micro-cell*

The micro-cell used in this work was filled with Rb vapor and neon buffer gas under pressure of about 100 Torr. The use of buffer gas was motivated by the results of [12, 13] where it was shown that for the formation of the EIT resonance in Λ-system using MC it is important to provide a small frequency detuning Δ of the coupling laser from the respective atomic transition. High magnetic field, however, results in high Δ. In such case, EIT occurs for the atoms moving in the laser-beam direction $z$ with the velocity $V_z = 2\pi\Delta/k$, where $k = 2\pi/\lambda$. That high $V_z$ reduces the time of flight $\tau = L/V_z$ and, consequently, increases the phase decoherence rate ($\Gamma_{12} = 1/2\pi\tau$) between two lower levels of the Λ-system. An increase in $\Gamma_{12}$ decreases the amplitude and broadens the EIT resonance. On the other hand, the presence of a buffer gas (~100 Torr) greatly reduces the mean free path of the alkali atoms (down to ~1 μm) such that they do not reach the walls of the 30 μm cell (this also increases the interaction time of the atom and laser light).

### *The Experimental Setup*

The scheme of the experimental setup is shown in Fig. 1. We used the radiation of two continuous wave narrowband extended cavity diode lasers (ECDL) with a wavelength of 795 nm and a spectral width of ~1 MHz. The coupling laser had the fixed frequency $\nu_C$, whereas the probe laser frequency $\nu_P$ was tunable. The polarization beam splitters PBS1 and PBS2 formed mutually perpendicular linear polarizations of the coupling and probe fields. Both beams with a diameter of ~1 mm were combined in the PBS[3] and directed to the studied cell.

A part of the probe $\nu_P$ radiation was directed to an auxiliary Rb NC (*6*). This cell was used as a frequency reference as described in [14]. The transmitted light was detected by standard FD-24K photodiodes (*5*). The photodiode signals were amplified by operational amplifiers and supplied to a Tektronix TDS2014B four-channel oscilloscope (*8*). The radiation of the coupling laser was partly directed to system (*7*) to form the error signal and stabilize frequency $\nu_C$ [15]. Magnetic fields under 200 G were produced by the system of Helmholtz coils (not shown in Fig. 1), into which the oven with the micro-cell was placed. Strong magnetic fields were produced by disk shaped permanent magnets with the diameter 60 mm, width of ~30 mm, and a 2 mm bore for the transmission of the laser beams. The permanent magnets were mounted onto two nonmagnetic stages with the possibility of gradually adjusting the distance between them. The magnetic field in the micro-cell increased when the permanent magnets approached each other (the technique of the measurement of the inhomogeneous magnetic field is described elsewhere [14]). The radiation of the coupling laser was cut off by the PBS4 so that merely the probe radiation was detected. For better selection of the probe radiation at a wavelength of 795 nm, an interference filter (IF) with a half-maximum bandwidth of 10 nm was used.

## EXPERIMENTAL RESULTS AND DISCUSSION

### *Nano-cell*

We have studied the Λ-system of the $D_1$-line of $^{85}$Rb atoms shown in the inset of Fig. 2. Here, the frequency $\nu_C$ is in resonance with the $F_g = 3 - F_e' = 3'$ transition (primed numbers stand for upper levels), whereas the frequency $\nu_p$ is swept through the $2 \rightarrow 2'$, 3' resonances. In the presence of the external longitudinal magnetic field $\mathbf{B} \parallel \mathbf{k}$ (where $\mathbf{k}$ is the wave vector of the laser field), several Λ-systems of different $m_F$ sublevels are formed (see Figs. 2, 3). The power of the coupling ($P_C$ = 1–30 mW) and probe ($P_P$ < 1 mW) lasers emission was chosen so that the EIT components were narrow and had high contrast. Figure 2 presents the probe transmission spectra *a*, *b*, *c* for magnetic fields $B$ = 55, 300, and 770 G, respectively; the curve *d* depicts the EIT resonance at $B = 0$, while *e* shows the spectrum of the velocity-selective optical pumping (VSOP) with the reference frequency interval of 362 MHz. The EIT components are marked by numbers *1–5* (this numbering is the same in Fig. 3 below). The frequency intervals between the high and low frequency components numbered *1* and *5*, respec-

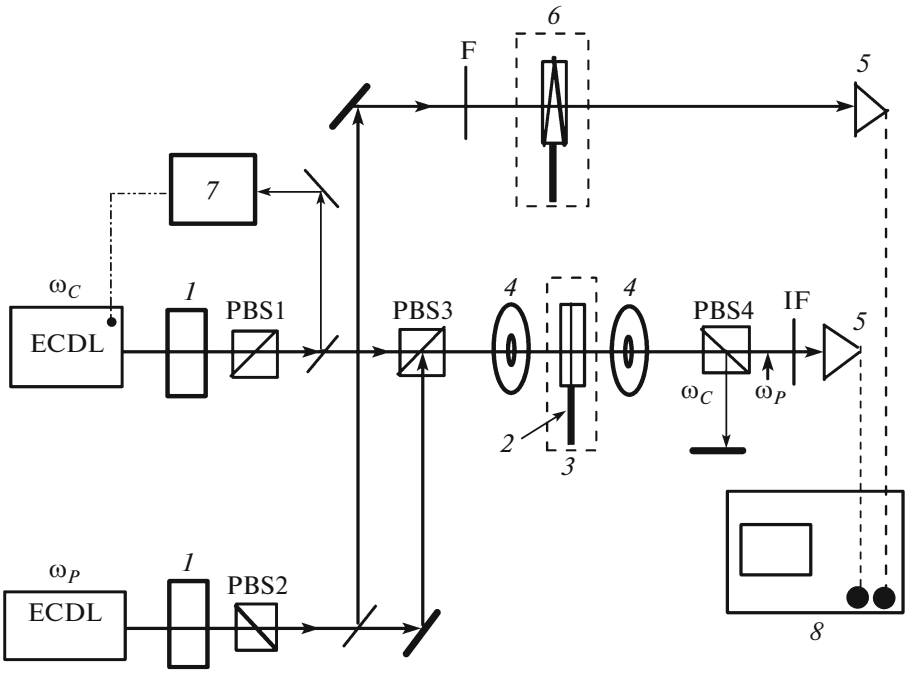


**Fig. 1.** Scheme of the experimental setup with the (ECDL) continuous wave narrowband extended cavity diode lasers with λ ≈ 795 nm and a spectral width of ~1 MHz: Faraday isolators (*1*), polarization beam splitters (PBS1, 2, 3, 4), cells filled with Rb (*2*), cell in the oven (*3*), permanent magnets (*4*), photodiodes (*5*), auxiliary Rb NC with the width $L = \lambda$ (*6*), frequency stabilization system (*7*), and 4-channel digital oscilloscope (*8*).

tively, increase with the magnetic field. At the same time, the amplitudes of the EIT components decrease gradually with an increase in the magnetic field. It is easy to show that in a longitudinal magnetic field five Λ-systems of atoms are formed involving the magnetic sublevels of the ground states $F_g = 2, 3$ (see inset in Fig. 3). Despite the fact that the amplitudes of the EIT components decrease with an increase of the magnetic field, the components are well resolved up to 1 kG. The magnetic-field dependent decrease of the amplitudes of the EIT components has two reasons: an increase in the magnetic field leads to an increase in the detuning Δ of the frequency $\nu_C$ from the respective atomic transition, and (more importantly [16]) a decrease of the atomic transition probabilities at frequencies $\nu_C$ and $\nu_P$ [17–19].

Thus, the use of NC allows formation and study of the EIT-components up to 1 kG (see below). It is important that the observed spectra are not obscured by the VSOP resonances that are present in the centimeter length cells [20]. Such VSOP resonances also split in a magnetic field, making it very difficult to distinguish all EIT-components.

From a practical point of view, the use of NC has great advantages when measurement of strongly nonuniform (gradient) magnetic fields is necessary, due to its sub-micron (~0.79 μm) spatial resolution.

*Micro-cells*

We investigated the same Λ-system of $^{85}$Rb atoms at the $D_1$ line (inset in Fig. 2) with a 30 μm-long microcell. The power of the coupling $P_C$ (1–30 mW) and probe $P_P$ (~1 mW) lasers was adjusted to detect weak EIT resonances in strong magnetic fields. The behavior of EIT in the $D_1$ line of $^{85}$Rb atoms, using 30-μm cell filled with Rb vapor and neon buffer gas (pressure of 100 Torr) in strong magnetic fields was first studied in [12]. Figure 3 shows the similar probe transmission spectra containing EIT resonances obtained in this work at magnetic field strengths 410, 704, and 1160 G (spectra *a*, *b* and *c* respectively), *d* shows the EIT resonance at zero magnetic field, and *e* is the reference spectrum. As can be seen, in a longitudinal magnetic field, the EIT resonance splits into five components, which may be recorded in a larger magnetic fields than that in the case of the NC. It is interesting to note that frequencies of the components *4* and *5* initially decrease—with increasing magnetic field, and then begin to increase, and at magnetic field $B = 722$ and 1444 G, respectively, are formed on the same frequency as the $B = 0$ EIT-resonance (see below). Importantly, using the buffer-gas-filled cells helps to avoid VSOP resonances which facilitates identification of EIT component. As noted in [12], the use of 30-μm cell with the addition of buffer gas allows the

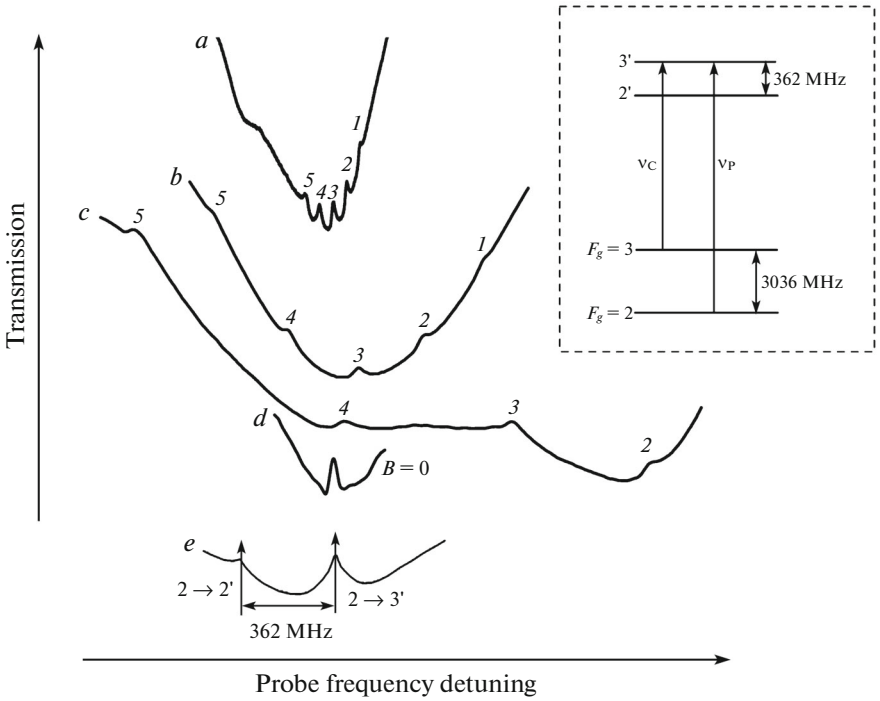


**Fig. 2.** Transmission spectra observed with the NC of $L \approx 795$ nm, (*a*, *b*, *c*) with $B = 55$ G (*a*), 300 G (*b*), 770 G (*c*), 0 G (EIT resonance, *d*). The spectra are shifted vertically for convenience; EIT-components are sequentially numbered as *1–5*. The temperature is 120°C. Configuration of the $\nu_C$ and $\nu_P$ is shown in dotted rectangle (the frequency $\nu_P$ scanned around $F_g = 2 \rightarrow 5P_{1/2}$ transition). The reference spectrum (*e*) was obtained with an additional Rb NC.

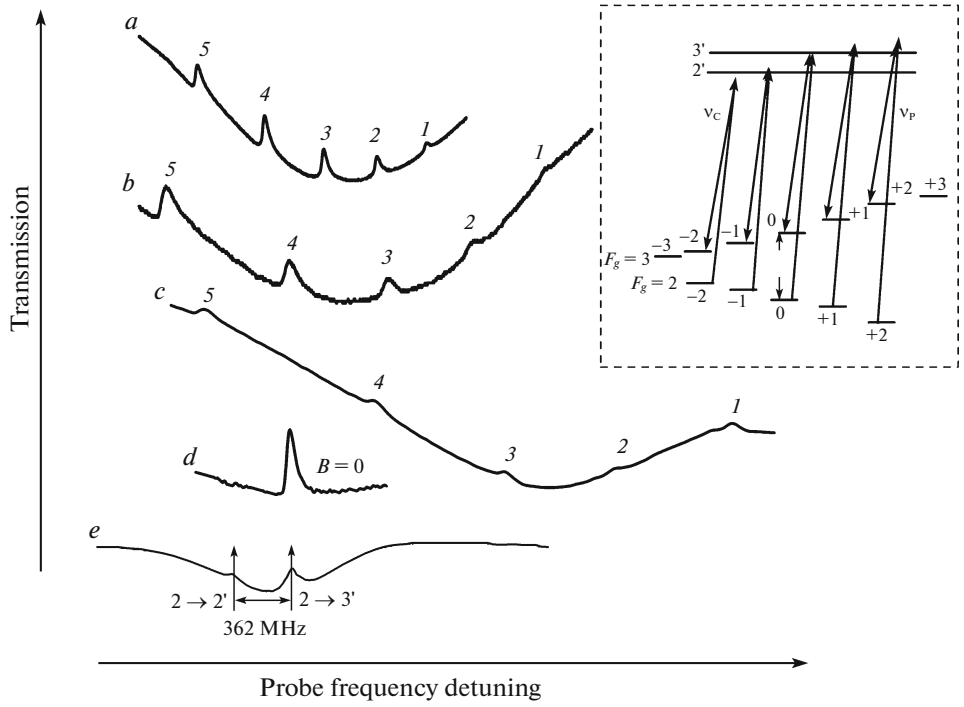


**Fig. 3.** Transmission spectra observed with a micro-cell of $L = 30$ μm at $B = 410$ G (*a*), 704 G (*b*), 1160 G (*c*), and 0 G (EIT resonance, *d*). The spectra are shifted vertically for convenience; EIT-components are sequentially numbered as *1–5*. Configuration of $\nu_C$ and $\nu_P$ is shown in dotted rectangle (frequency $\nu_P$ scanned around $F_g = 2 \rightarrow 5P_{1/2}$ transition). The reference spectrum (*e*) was obtained with an additional Rb NC.

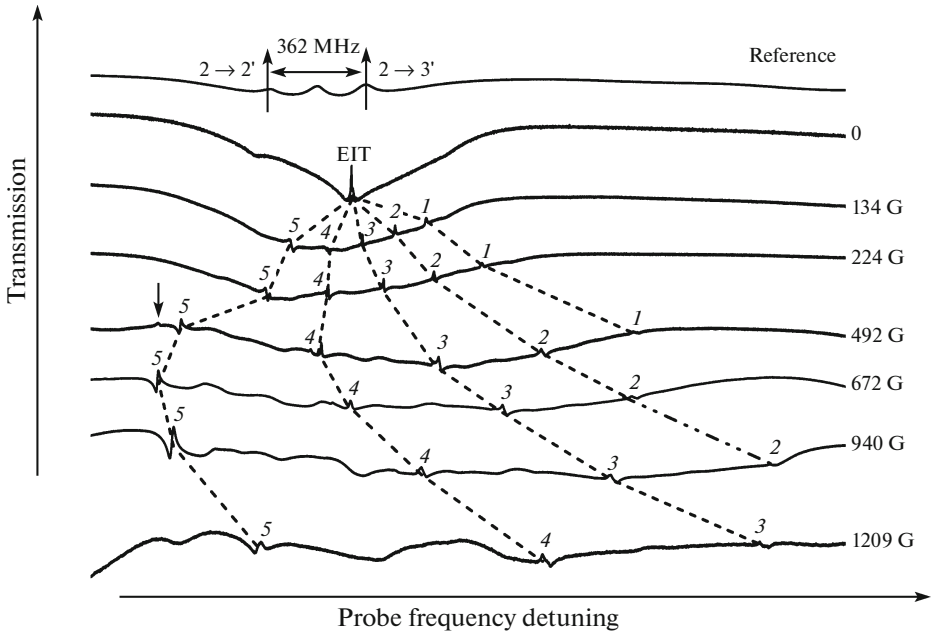


**Fig. 4.** Transmission spectra containing EIT resonances under various magnetic fields observed with the centimeter-cell of $L$ = 0.8 cm. The power of the coupling and the probe lasers is 8 mW and 0.2 mW, respectively, the temperature is 40°C. The dotted lines connect the positions of the *1–5* components on magnetic field (the vertical positions of individual spectra are arbitrary, so the dotted lines do not reproduce exactly the energy level dependence on $B$). Note that for some values of the magnetic field small EIT-satellites appear (shown with the arrow).

formation and study of the EIT -components up to 1.8 kG.

From a practical standpoint the use of 30-μm cell allows one to form narrow optical resonances strongly frequency shifted (relative to the unperturbed atomic transitions) which can be used, particularly, for the laser frequency stabilization [6].

### *Centimeter-long Cells*

Here, the results of the study of EIT resonances in high magnetic field using conventional centimeter-long glass cells are presented for the first time. The absence of other similar work is caused by the technical difficulty of producing strong homogeneous magnetic fields of a few kG at centimeter lengths (the system has been assembled in the Jagiellonian University, Krakow). We investigated the same Λ-system as in Fig. 2 inset. Figure 4 shows the transmission spectra of the probe beam containing five EIT resonances, for magnetic field increasing from zero (the second curve from the top) to 1209 G (lower curve). We used the 0.8 cm-long glass cell filled with Rb, and the oven temperature was 40°C. The upper curve shows the reference spectrum of saturated absorption. In this case, when $B = 0$, a narrow 3.5 MHz wide (FWHM) EIT resonance is formed, narrower than the natural width (~6 MHz). As can be seen from the spectra, in some cases the EIT resonances have dispersion profile that we attribute to the competition of the EIT and other Raman-like processes [21]. The VSOP resonances that have larger spectral width than the sub-natural EIT-components are also visible in the spectra. Application of the 0.8 cm-cell allows for formation and study of the EIT-components up to 1.4 kG. Note that for some values of the magnetic field, small EIT-satellites appear, as shown with the arrow in Fig. 4.

The necessary condition to form EIT-resonances in magnetic field is $\nu_P - \nu_C = [E(F = 3, m_F) - E(F = 2, m'_F)]/h$ [3, 12], for the relevant Zeeman sublevels of the ground states $F_g = 2, 3$ (see inset in Fig. 2). The energies of the Zeeman sublevels can easily be calculated as, e.g. in [17, 19]. Figure 5 shows the calculated curves (solid lines) for the EIT-components with the numbers *1–5* corresponding to the configuration of the $\nu_P$ and $\nu_C$ frequencies, such as shown in the inset in Fig. 2, while the small EIT-satellites are associated with the curve *6*. Note that at strong magnetic fields the satellites disappear. The symbols represent the experimental results. The numbers on the right indicate the Zeeman sublevels which are involved in the EIT resonance formation (see the inset in Fig. 3): the first number indicates sublevel $m'_F$ of the ground level $F_g = 2$, and the second number indicates sublevel $m'_F$ of the ground level $F_g = 3$. Note that for some sublevel-configurations, like ($m_F = 0$, $m'_F = 2$) and ($m_F = 2$, $m'_F = 0$), the probe frequencies $\nu_P$ coincide. As seen in Fig. 5, the EIT components with $m'_F - m_F = 0$ survive

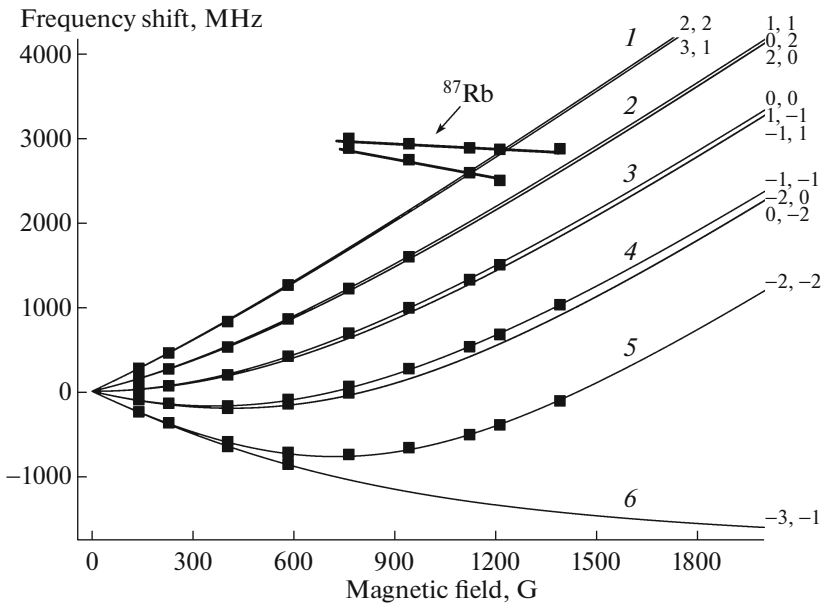


**Fig. 5.** The dependence of the frequency shifts of EIT-components (frequencies configuration of $\nu_C$ and $\nu_P$ is shown in the inset of Fig. 2) on the magnetic field. Solid lines are the calculated curves; the symbols are experimental points. When $B > 1$ kG, the slopes of the curves *1–5* (the numbering corresponds to EIT-components in Figs. 2, 3) are positive, and the slope values asymptotically approach $s = 2.8$ MHz/G, which is the manifestation of the HPB regime. Within the range of laser tuning, some EIT resonances belonging to $^{87}$Rb are visible.

at higher fields. Each of these components is formed by the two pairs of the coupling and probe radiations corresponding to two helicities of both light beams $(\sigma_P^+,\sigma_C^+)$ and $(\sigma_P^-,\sigma_C^+)$. The previously observed (Figs. 2, 3) frequency dependence of the EIT components versus the magnetic field $B$ is in good agreement (the inaccuracy is within 2%) with the theory. The frequency slopes (the derivative of the frequency shifts) of all curves becomes positive at $B > 1$ kG and asymptotically approaches $s \approx 2.8$ MHz/G.

This behavior is due to the fact that at $B > 1$ kG the total angular momentum **J** of the electron and nuclear magnetic moment **I** starts to decouple and the behavior of atomic levels perturbed by the magnetic field are described by projections $m_J$ and $m_I$ (so-called Paschen-Back or Back-Goudsmit regime of the hyperfine structure (HPB)): the behavior of the Zeeman sublevels of $F_g = 2, 3$ are shown, for example, in [22–24]. The values of the magnetic fields where the **I**–**J** decoupling is efficient are determined by the condition $B \gg B_0 = A_{HFS/\mu B}$, where $A_{HFS}$ is the hyperfine coupling constant for the $5S_{1/2}$ ground state of Rb and $\mu_B$ is the Bohr magneton (appropriate values are given e.g. in [25]). The $B_0$ value for the $^{85}$Rb atoms is ~0.7 kG. Note that at $600 < B < 800$ G some satellites appear in five EIT resonances, which is consistent with the theory. Interestingly, in the range of $700 < B < 1400$ G additional EIT resonances appear generated with frequencies $\nu_C$ and $\nu'_P$ in the $D_1$ line of $^{87}$Rb, while the frequency $\nu'_P$ is close to the frequency of the *1–1'*, *2'* transitions.

For the sake of comparison, the 2.5 cm-long glass cell filled with Rb vapor was also used. In this case for $B > 1$ kG the generated EIT resonances had a lower contrast and signal/noise ratio as compared with the thin (0.8 cm) cell.

## CONCLUSIONS

A comparison of the experimental results on the formation of the EIT resonances in strong magnetic fields was obtained using three different types of spectroscopic cells:

(1) nano-cells filled with Rb vapor with the thickness of $L = 795$ nm. Application of NC allows for the formation of EIT-components up to 1 kG, using readily available permanent magnets. There are no VSOP resonances in the spectra which is convenient for spectrum processing. From a practical point of view, the use of NCs provides sub-micron spatial resolution suitable for measurements of strongly non-uniform magnetic fields;

(2) Rb micro-cell of a 30 μm thickness with the addition of buffer gas. This cell enables the formation and the study of the EIT components up to 1.8 kG. From a practical standpoint the use of micro-cells allows one to form highly detuned narrow optical resonances, which can be used for laser frequency stabilization;

(3) Rb glass cell of a centimeter lengths. By comparing two cells with 0.8 and 2.5 cm length it was discovered that the shorter one yields better spectra. The EIT resonances recorded with the cm-cells are narrower than the resonances generated in NC and MC. Another advantage is the ease of manufacturing such glass cells. The disadvantage is the non-trivial formation of magnetic fields sufficiently homogenous within a large volume, as well as the presence of VSOP resonances, which are making difficult both the detection and correct assignment of the EIT components.

In conclusion, all three types of applied cells are suitable for the observation of Paschen-Back/Back-Goudsmit regime of the hyperfine structure.

The authors thank A.S. Sarkisyan for the cells fabrication. This research was supported by a Marie Curie International Research Staff Exchange Scheme Fellowship, FP7 "Coherent optics sensors for medical applications—COSMA," POIG 02.01.00-12-023/08, and NCN (2012/07/B/ST2/00251). R.M. thanks Jagiellonian University, Krakow for the possibility to work in very nice conditions and for the hospitality. A.S. and D.S. gratefully acknowledge the financial support of the State Committee for Science of the Ministry of Education and Science of the Republic of Armenia in the framework of project № 15T-1C040.

## REFERENCES

1. K.-J. Boller, A. Imamoglu, and S. E. Harris, Phys. Rev. Lett. **66**, 2593 (1991).
2. J. E. Field, K. H. Hahn, and S. E. Harris, Phys. Rev. Lett. **67**, 3062 (1991).
3. M. Fleischhauer, A. Imamoglu, and J. P. Marangos, Rev. Mod. Phys. **77**, 633 (2005).
4. J. Vanier, Appl. Phys. B **81**, 421 (2005).
5. E. B. Aleksandrov, Phys. Usp. **53**, 487 (2010).
6. A. Sargsyan, A. Tonoyan, R. Mirzoyan, et al., Opt. Lett. **39**, 2270 (2014).
7. X. Wei, J. Wu, G. Sun, et al., Phys. Rev. A **72**, 023806 (2005).
8. S. Mitra, S. Dey, M. M. Hossain, et al., J. Phys. B: At. Mol. Opt. Phys. **46**, 075002 (2013).
9. A. Sargsyan, R. Mirzoyan, and D. Sarkisyan, Opt. Spectrosc. **113**, 456 (2012).
10. D. Sarkisyan, D. Bloch, A. Papoyan, and M. Ducloy, Opt. Commun. **200**, 201 (2001).
11. J. Keaveney, A. Sargsyan, U. Krohn, et al., Phys. Rev. Lett. **108**, 173601 (2012).
12. A. Sargsyan, R. Mirzoyan, and D. Sarkisyan, JETP Lett. **96**, 303 (2012).
13. A. Sargsyan and D. Sarkisyan, Opt. Spectrosc. **111**, 334 (2010).
14. A. Sargsyan, G. Hakhumyan, A. Papoyan, et al., Appl. Phys. Lett. **93**, 021119 (2008).
15. A. Sargsyan, A. Papoyan, D. Sarkisyan, et al., Eur. Phys. J. Appl. Phys. **48**, 20701 (2009).
16. A. Sargsyan, Y. Pashayan-Leroy, C. Leroy, et al., J. Mod. Opt. **62**, 769 (2015).
17. A. Sargsyan, G. Hakhumyan, C. Leroy, et al., J. Opt. Soc. Am. B **31**, 1046 (2014).
18. A. Sargsyan, A. Tonoyan, G. Hakhumyan, et al., Opt. Commun. **334**, 208 (2015).
19. E. B. Aleksandrov, G. I. Khvostenko, and M. P. Chaika, *Interference of Atomic States* (Nauka, Moscow, 1991) [in Russian].
20. A. Sargsyan, D. Sarkisyan, D. Staedter, and A. M. Akulshin, Opt. Spectrosc. **101**, 762 (2006).
21. C. Hancox, M. Hohensee, M. Crescimanno, et al., Opt. Lett. **33**, 1536 (2008).
22. A. Sargsyan, G. Hakhumyan, C. Leroy et al., Opt. Lett. **37**, 1379 (2012).
23. L. Weller, K. S. Kleinbach, M. A. Zentile, et al., Opt. Lett. **37**, 3405 (2012).
24. A. Sargsyan, R. Mirzoyan, T. Vartanyan, D. Sarkisyan, J. Exp. Theor. Phys. **118**, 359 (2014).
25. M. A. Zentile, J. S. Keaveney, L. Weller, et al., Comput. Phys. Commun. **189**, 162 (2015).